Gravitational waves searches

Claudia Lazzaro - Virgo group
Seminar 12 April 2017
Experimental astroparticle physics

Gravitational waves and General Relativity

- Gravity is a manifestation of curvature of space-time produced by matter-energy
- Linearized Einstein equations admit wave solutions, as perturbations to a background geometry. $g_{\nu\mu}=\eta_{\nu\mu}+h_{\nu\mu}$ $h_{\nu\mu}\ll 1$

- Any rapidly moving mass generates fluctuations in spacetime curvature which propagate at the speed of light.

Gravitational waves

- Propagate with speed of light,
- Transverse, traceless
- Have two independent polarizations states “+” and “x”
- Can be detected by their effect on the relative motion of test masses (stress and compress spacetime in two directions)

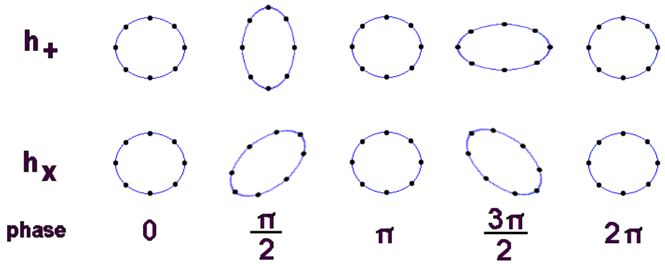

$$\boxed{\frac{\Delta L}{L}\sim h}$$

GW existence: Hulse and Taylor binary

GW emission has been indirectly demonstrated through the radiative energy loss of PSR191316

- ✗ Pulsar bound to a “dark companion”, 7kpc from Earth. (vmax/c ~10--3)
- ✗ GR predicts such a system to lose energy via GW emission: orbital period decrease
- ✗ Prediction of general relativity verified at 0.2% level

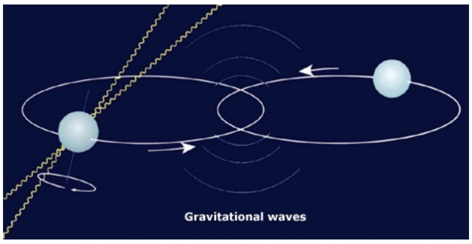

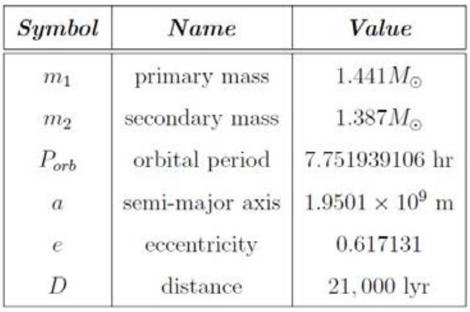

Symbol	Name	Value
m_1	primary mass	$1.441 M_\odot$
m_2	secondary mass	$1.387 M_\odot$
P_{orb}	orbital period	7.751939106 hr
a	semi-major axis	1.9501×10^9 m
e	eccentricity	0.617131
D	distance	21, 000 lyr

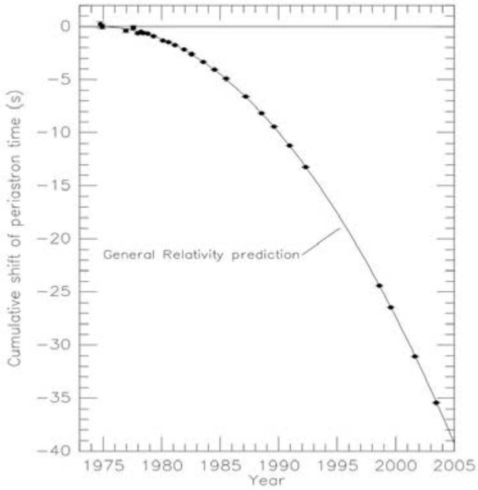

GW amplitude

Mass quadrupole $Q_{\mu\nu}$

Radiated power $P = \frac{G}{5c^2} \dddot{Q}_{\mu\nu} \dddot{Q}^{\mu\nu}$

Amplitude $h_{\mu\nu} = \frac{2G}{c^4} \frac{1}{r} \dddot{Q}_{\mu\nu}$

$\dddot{Q}_{\mu\nu} != 0$

Efficient sources of GW must be asymmetric, compact and fast

GW detectors are sensitive to amplitude

h: 1/r attenuation

Possible GW source:

Transient signal from core collapse supernovae:

$$h \sim 6 \times 10^{-21} \left(\frac{E}{10^{-7}\,\mathrm{M}_\odot c^2} \right)^{\frac{1}{2}} \left(\frac{1\,\mathrm{ms}}{T} \right) \left(\frac{1\,\mathrm{kHz}}{f} \right) \left(\frac{10\,\mathrm{kpc}}{r} \right)$$

Continuous waves from non asymmetric spinning neutron stars

$$h_0 = \frac{4\pi^2 G I_{zz} f_{GW}^2}{c^4 r} \epsilon = (1.1 \times 10^{-24}) \left(\frac{I_{zz}}{I_0} \right) \left(\frac{f_{GW}}{1\,\mathrm{kHz}} \right)^2 \left(\frac{1\,\mathrm{kpc}}{r} \right) \left(\frac{\epsilon}{10^{-6}} \right) \qquad \epsilon \equiv \frac{I_{xx} - I_{yy}}{I_{zz}}$$

Even in optimistic case: $h \leqslant 10^{-20}$

Need to measure: ΔL ~ 10^{-18} m

Michelson e Morley interferometers

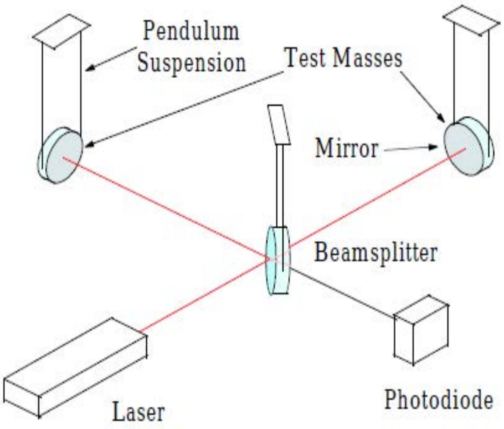

- ✗ Suspended mirrors act as “test-particles” (in “free-fall”)
- ✗ Sensitivity increases with L, then arms have kilometric scales length
- ✗ Laser beam is separated at the beamsplitter, in perpendicular directions. The light reflected on the mirrors returns backs and is collected to the photodetector
- ✗ Interferometer works in the dark fringe

$$\Delta\phi = 4\pi \frac{L h_+}{\lambda_{Laser}} \frac{\sin\left(\frac{\omega_{GW} L}{c}\right)}{\frac{\omega_{GW} L}{c}}$$

- ✗ Cut-off frequency $\Omega_{GW} L \sim \frac{\pi}{2} \Rightarrow L < \frac{\lambda_{\Omega_{GW}}}{4}$
- ✗ Broad-band response ~10 Hz to few kHz

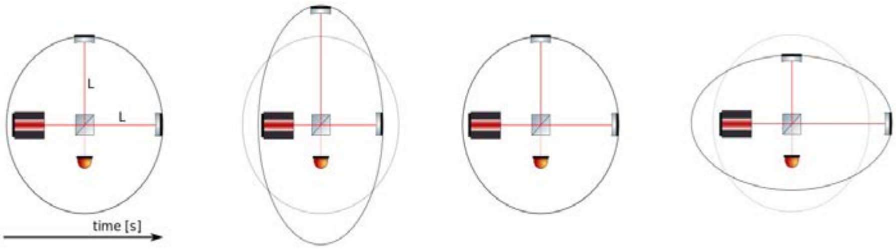

Interferometer response to h_+ .
Anisotropic response and polarization sensitivity

Interferometers

Improving the sensitivity: Increase length of the interferometer arms, increase incident light power
Reaching h~10-22 would requires, kilometric arms scale and kilowatts of laser power

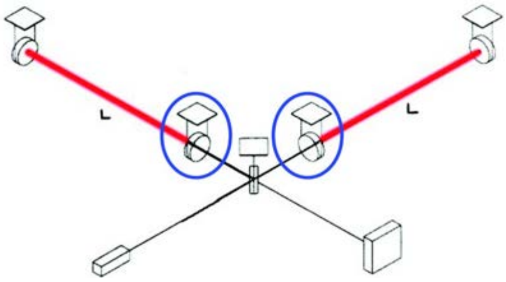

Fabry-Perot cavities

Effective light path length increased
Gain factor for Advanced Virgo ~300

Power recycling

$$P_{eff} = P_i * Recycling\ factor$$

Add recycling mirror between the input laser and the beamsplitter IFO, highly reflecting mirrors
gain~40 for Advanced Virgo

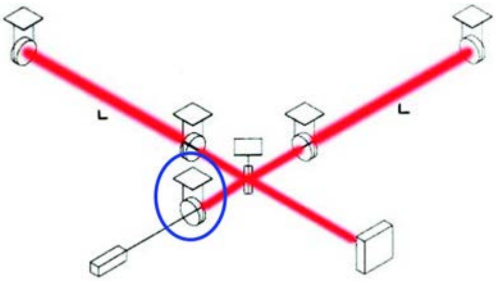

Additional improvement: Signal recycling mirror to be added in front of the dark port

Interferometers: optical layout

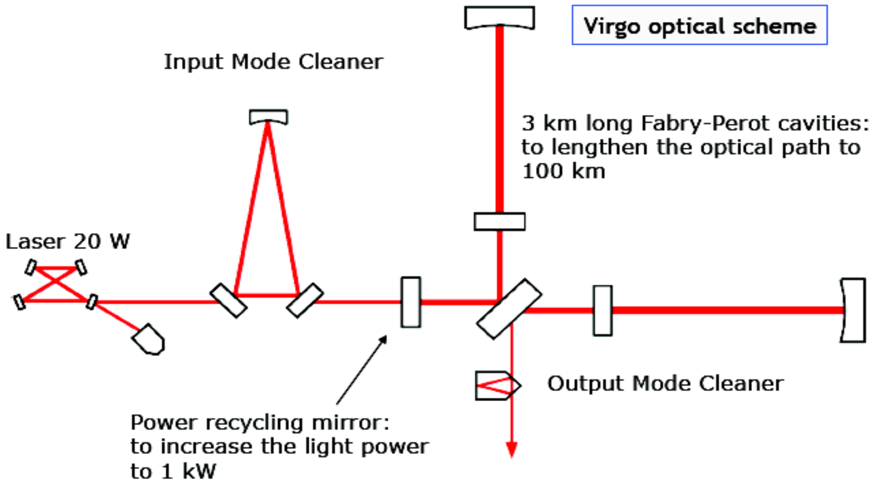
Virgo optical scheme

Input Mode Cleaner

3 km long Fabry-Perot cavities: to lengthen the optical path to 100 km

Laser 20 W

Output Mode Cleaner

Power recycling mirror: to increase the light power to 1 kW

Operation conditions (Locking conditions):

- Keep the FP Cavities In resonance (Maximize the phase response);
- keep the PR cavity in resonance (Minimize the shot noise);
- Keep the output on the “dark fringe” (Reduce the dependence on power fluctuations)

-Keep the arm length constant within 10-15 m

AdvVirgo interferometer

Arms:

3km length

Vaccum volume 7000 m^3 , 10^{-9} mbar

AdvVirgo interferometer

Arms:
3km length
Vaccum volume 7000 m^3 , 10^{-9} mbar

Suspension
Super-seismic isolation (from initial Virgo)
Reduction 10^{-12} vibrations

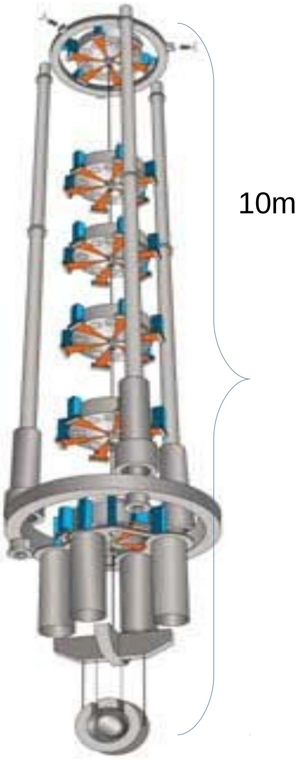

AdvVirgo interferometer

Arms:
3km length
Vaccum volume 7000 m^3 , 10^{-9} mbar

Suspension
Super-seismic isolation (from initial Virgo)
Reduction 10^{-12} vibrations

Mirrors

✗ 42 kg, 35 cm diam., 20 cm thick
✗ Flatness < 0.5 nm rms
✗ Roughness < 0.1 nm rm
✗ Absorption < 0.5 ppm
✗ Low mechanical losses, Low optical absorption

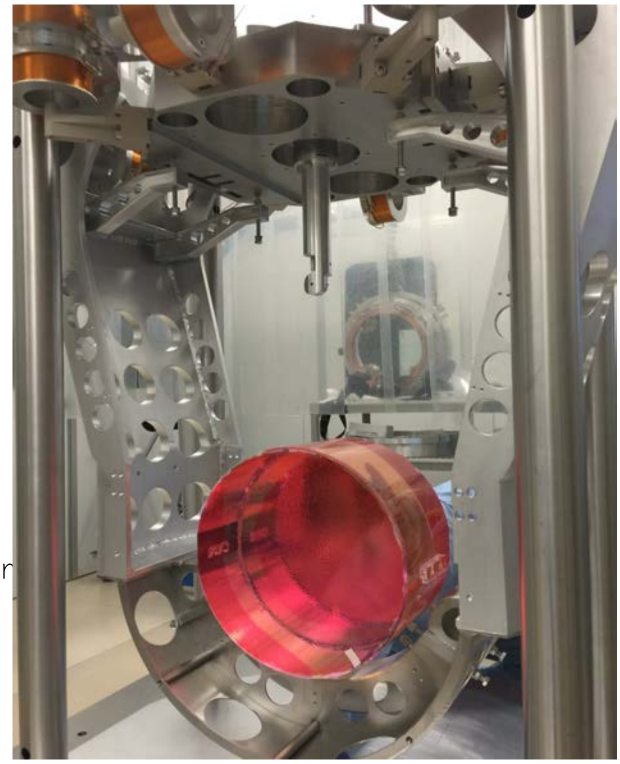

Ground based interferometers: main noise source

IFO sensitivity: power spectrum density (PSD, unit: 1/√Hz)

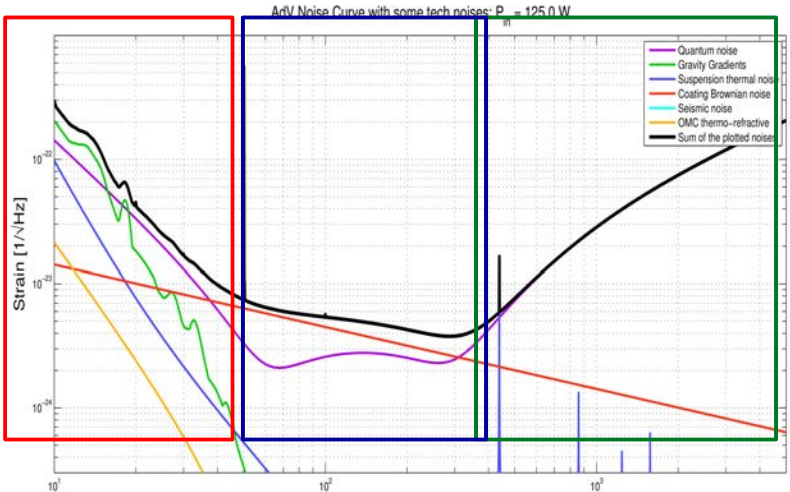

Fundamental Noise Sources:

- ✗ Seismic noise
- ✗ Newtonian noise/Gravity gradients
- ✗ Radiation pressure noise

- ✗ Thermal noise
- ✗ Mirror coatings
- ✗ Mirror substrates

- ✗ Quantum shot noise

- ✗ Seismic noise strongly suppressed by properly designed suspension systems).
- ✗ The two main thermal noise sources: wires suspending mirrors and mirrors themselves (mainly optical coatings on mirrors surface)
- ✗ Photon shot noise is due to the quantum nature of the light; it arise from statistical fluctuations in the number of detected photons.

Network of interferometers

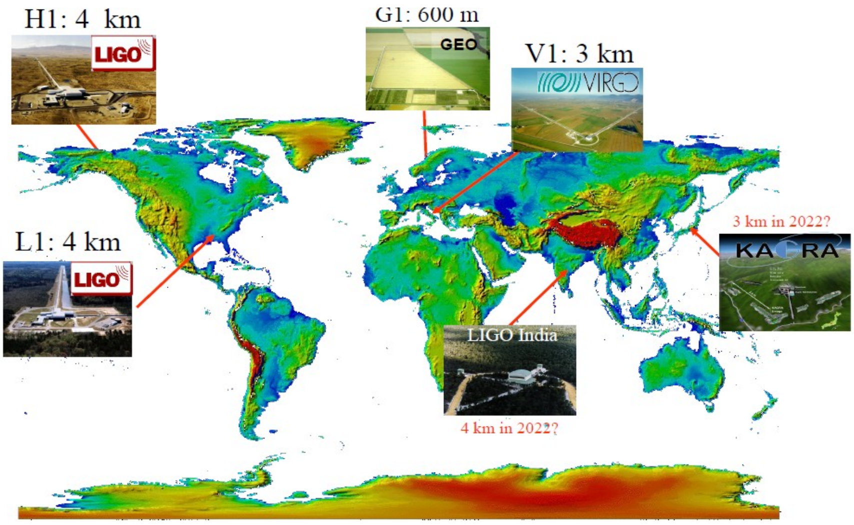

Data taking:
-LIGO Hanford (H1)
-LIGO Livingston
Upcoming:
-Virgo
Future:
-Kagra (2021)
-Ligo India (2022)

Advantages of multiple interferometer:

- ✗ Simultaneous detection, improve background rejection and detection confidence
- ✗ Duty cycle
- ✗ Enhanced network sky coverage, source parameter estimation(position and polarization)

Detector response to GW signal

Interferometer has non-uniform response in the sky

Direction to the source **θ,ϕ** and polarization angle **Ψ** define relative orientation of the detector and wave frames.

$$F_+ = \frac{1}{2}(1+\cos^2\theta)\cos 2\phi \cos 2\psi - \cos\theta \cos 2\phi \cos 2\psi$$

$$F_x = \frac{1}{2}(1+\cos^2\theta)\cos 2\phi \sin 2\psi + \cos\theta \cos 2\phi \cos 2\psi$$

$$h(t) = F_+(\theta,\phi,\psi)h_+ + F_x(\theta,\phi,\psi)h_x$$

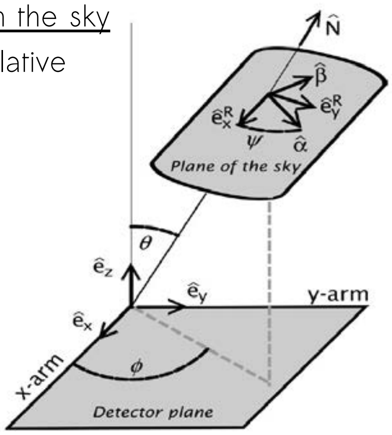

Astro-ph arXiv:1102.5421v2

F+ and F× antenna pattern depend on the source position in the sky and the interferometer plane:

- Maximal when perpendicular to this plane
- Blind region in the sky

Detector data: $x(t) = h(t) + n(t)$

Interferometer response to GW signal

noise

Amplitude GW wave

$$h^2 = \int h_+^2 + h_x^2$$

Interferometers network response to GW signal

Multiple detector allows, improves:

- network sky coverage
- Source parameter estimation, polarization resolution

Network data allows coherent (not only coincident) analysis

Network response:

$$\begin{bmatrix} x_1 \\ x_2 \\ \vdots \\ x_N \end{bmatrix} = \begin{bmatrix} F_1^+ & F_1^\times \\ F_2^+ & F_2^\times \\ \vdots & \vdots \\ F_N^+ & F_N^\times \end{bmatrix} \begin{bmatrix} h_+ \\ h_\times \end{bmatrix} + \begin{bmatrix} n_1 \\ n_2 \\ \vdots \\ n_N \end{bmatrix}$$

Localization of the source position:

- Triangulation: measure time of flight with 2 or more detector sites and reconstruct ToF rings
- degeneracy along the rings can be reduce by using variability of antenna pattern

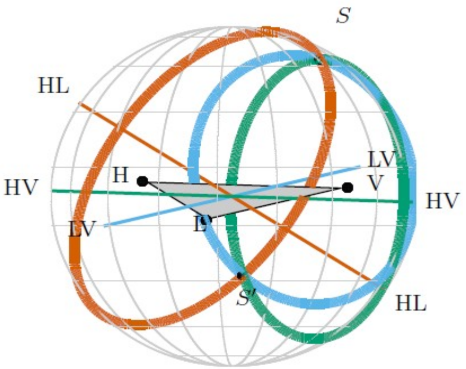

Interferometers network response to GW signal

How describe the coverage capability of the network:

- ✗ Network sensitivity $S_{net}=\left(\sum_k S_k^{-1}\right)^{-1}$
- ✗ Network acceptance $F=\sqrt{|F_+^2|+|F_x^2|}S_{net}$
- ✗ Network alignment $A=|f_x|/f_+$

Mean F

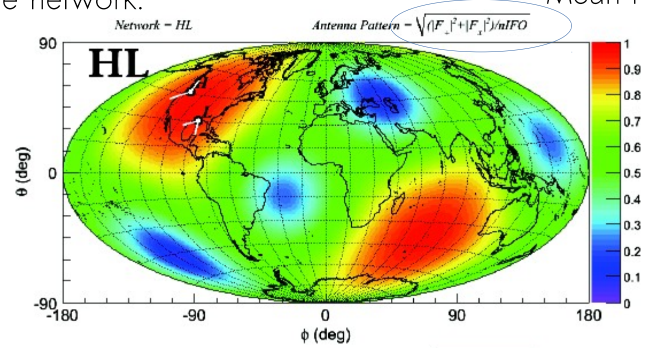

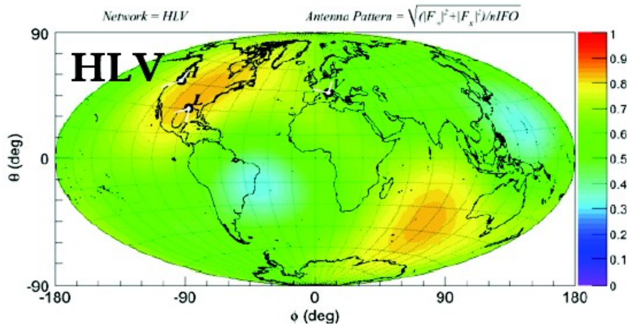

- ✗ multiple detectors improve coverage of the sky (acceptance & alignment) and strain sensitivity
- ✗ Even sensitive detectors, depending on source position, can act as spectator and not really participate in the measurement of event reconstruction
- ✗ Detectors with low sensitivity gives smaller contribution to the network SNR

NB: Hanford and Livigston are almost co-aligned

Interferometers network response to GW signal

...even 3 interferometers are not enough

LIGO H1+LIGO L1

$|\vec{F}_+|$

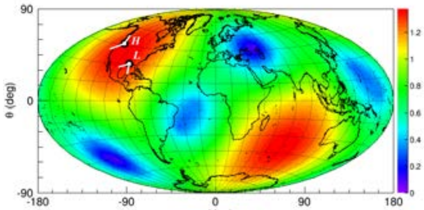

$|\vec{F}_\times|$

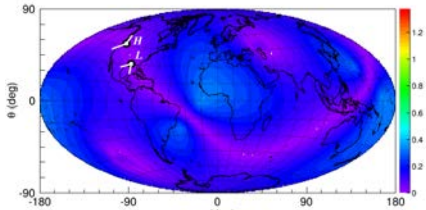

LIGO H1+LIGO L1+**Virgo**

$|\vec{F}_+|$

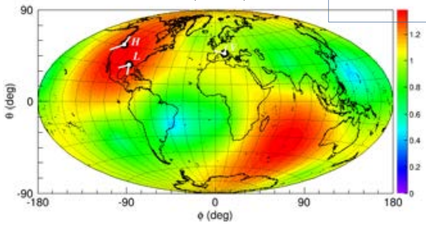

$|\vec{F}_\times|$

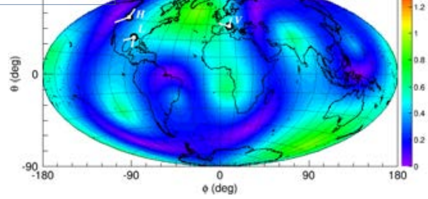

Astrophysical sources

Transient signals

Coalescing Compact Binary Systems (Neutron Star-NS, Black Hole-NS, BH-BH): Strong emitters, well modeled

Well known signals
Template search

Asymmetric Core Collapse Supernovae weak emitters, not well-modeled ('bursts'), transient
Cosmic strings, soft gamma repeaters,
pulsar glitches

Not known signals
burst search

Cosmological stochastic background (residue of the Big Bang, cosmic GW background, long duration)
Astrophysical stochastic background

Continuous signals

Spinning neutron stars (monotonic waveform, long/continuous duration)

known signals

Astrophysical sources

Transient signals

Coalescing Compact Binary Systems (Neutron Star-NS, Black Hole-NS, BH-BH): Strong emitters, well modeled

CBC search

Well known signals
Template search

Asymmetric Core Collapse Supernovae weak emitters, not well-modeled ('bursts'), transient
Cosmic strings, soft gamma repeaters,
pulsar glitches

Burst search

Not known signals
burst search

Cosmological stochastic background (residue of the Big Bang, cosmic GW background, long duration)
Astrophysical stochastic background

Stocastic search

Continuous signals

Spinning neutron stars (monotonic waveform, long/continuous duration)

known signals

Continuous search

CBC source

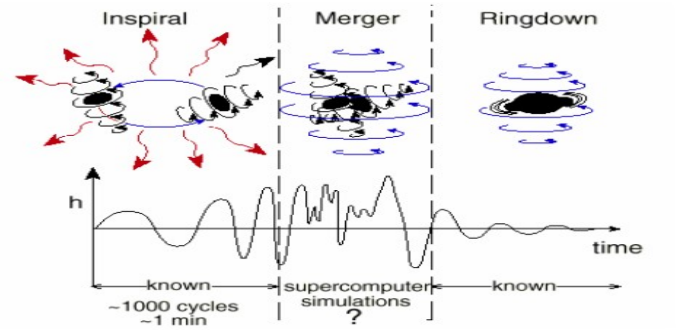

GW signal:
- ✗ Inspiral
- ✗ Merge
- ✗ ringdown

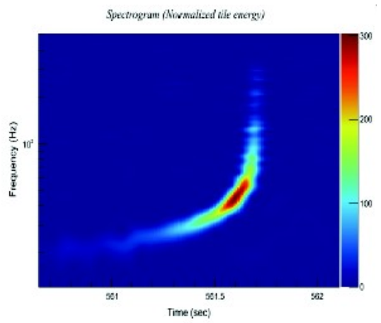

Till the ISCO (inner most circle orbital) characteristic frequency evolution in time: chirp signal

$$M_{chirp}=\frac{m_1 m_2^{3/5}}{m_1+m_2^{1/5}} \qquad \dot{f}_{GW}=\frac{96}{5}\pi^{8/3}\left(\frac{GM_c}{c^3}\right)^{5/3} f_{GW}^{11/3}$$

The GW emission is not isotropic, it depends on line of sight and luminosity distance

$$h_+=\frac{1}{D_L}\left(\frac{5}{c(t_c-t)^{1/4}}\right)\frac{1+cosi^2}{2}\cos[\Phi(t_c-t)] \qquad h_x=\frac{1}{D_L}\left(\frac{5}{c(t_c-t)^{1/4}}\right)cosi\sin[\Phi(t_c-t)]$$

Inclination of the orbital plane ɩ *& luminosity distance D_l*

CBC (template) search

Need to build a bank of template that will cover the full parameter space:

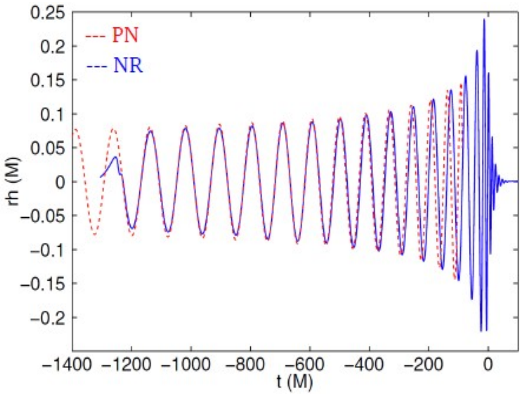

- ✗ To accurately calculate inspiral, merger and ring-down stage, “hybrid” waveforms are built. Post Newtonian approximation (PN) used for inspiral phase, Numerical relativity and perturbative theory for merger and ringdown phase
- ✗ Source parameters are encoded In detected waveforms., up to 15 parameters to include/estimate (chirp mass, component masses, spins,
- ✗ template not fully available for complex systems such as eccentric compact binaries, spinning ...

Template analysis search, main step (generic):

- ✗ matching filter for each template, find template that maximized matching template
- ✗ Same templates which are coincident in time (among the detector, including consistent time difference between sites) are combined in one event
- ✗ coincident triggers are ranked according to a detection statistic (combined SNR, weighted likelihood, ...)

Burst sources

Possible sources

- core-collapse supernovae
- CBC signal: the merger phase of binary compactobjects. In particular the burst search is crucial for eccentric binary black holes, and high precessing, spinning system; in this cases the template are not well known.
  Post merger phase of NS-NS phase (equation of state of NS)
- neutron star instabilities, pulsar glitches
- accretion disk instabilities
- cosmic string cusps/kinks,
- ....the un-expected

Waveform morphologies is poorly modeled or fully unknown.
Short duration signal: hundreds milliseconds to a few seconds
Long duration: signals lasting from few seconds up to hours

Burst searches

Burst search is performed without assumption (or minimal) on the phase evolution of the signal
Goal: cover wide range of parameters space (can overlap the modeled searches)

Burst analysis search, main step (generic):

- make time-frequency representation of the data, weight data by the noise at each frequency (whitening). Search for excess power in time-frequency domain, coincidently/coherently in different detectors data (considering time delay between detector sites and different antenna patterns of the detectors for any incoming direction).
- Coherent analysis of the triggers and estimation of the signal parameters. Different algorithms
- Ranked statistic

Joint GW and high-energy astrophysics

GWs and photons provide complementary information on the astrophysics source (and maybe on the environment)

Gravitational waves signal ⟺ Electromagnetic signal

Two scenario:

➔GW triggered EM follow-up: low-latency GW data analysis pipelines promptly identify GW candidates and send GW alerts to trigger prompt EM observations

Low latency analysis, GW candidates, skymap ~minutes → Event validation Hours, days → EM followup

➔EM triggered GW: an EM transient event is detected and GW triggered searches are are performed to look for possible associated GW events.

➔even more: joint with neutrino, searches neutrino candidates with data of IceCube and ANTARES

Joint GW and EM, astrophysics motivation

Coalescence of binary systems of NSs and/or BHs

- Short GRBs:

  Prompt γ-ray emission (< 2 s)

  Multiwavelegth afterglow emission: X-ray, optical and radio (minutes, hours, days, months).

-Kilonova: optical (days-weeks).

Core collapse of massive stars:

Supernovae:

-X-rays, UV (minutes, days)

-optical (week, months)

-radio (years)

Long GRBs (massive rapidly spinning star Collapse ??)

Isolated neutron stars

-soft γ–ray repeaters

-radio/X-ray pulsar glitches

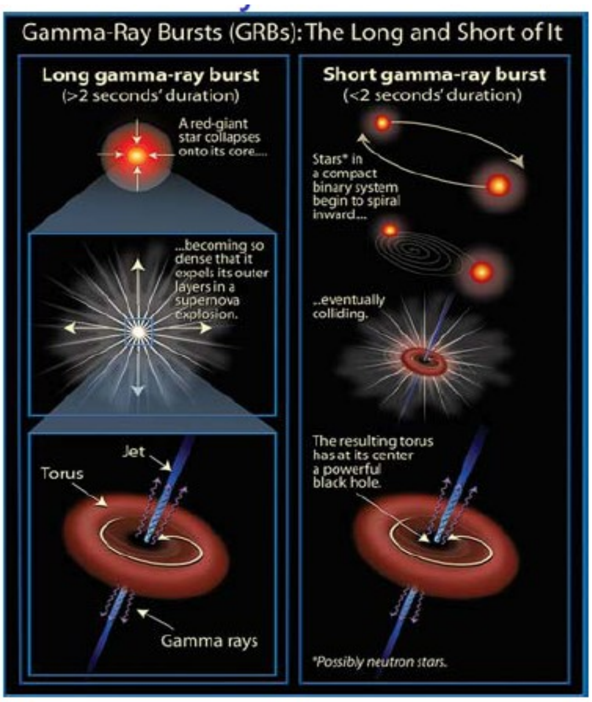

O1 data talking and sensitivity

September 12, 2015 - January 19, 2016
Total coincidence analysis time: 51.5 days
Total coincidence analysis time after removing noisy data: 48.6 days (~38%)

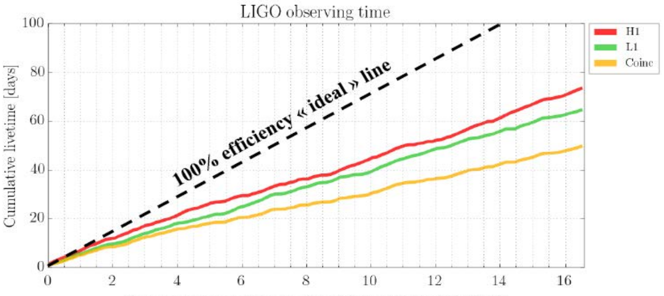

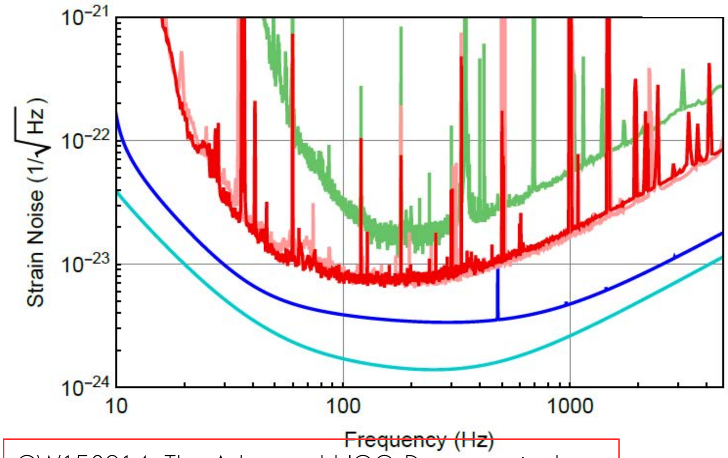

strain sensitivity during the First observation run (O1) of the Advanced LIGO detectors and during the last science run (S6) of the initial LIGO detectors.

– Hanford
– Livingston
– S6
– AdvancedLigo
(design sensitivity)

GW150914: The Advanced LIGO Detectors in the Era of FirstDiscoveries (Phys. Rev. Lett. 116,131103)

O1 analysis: binary black holes

Phys. Rev. X 6, 041015

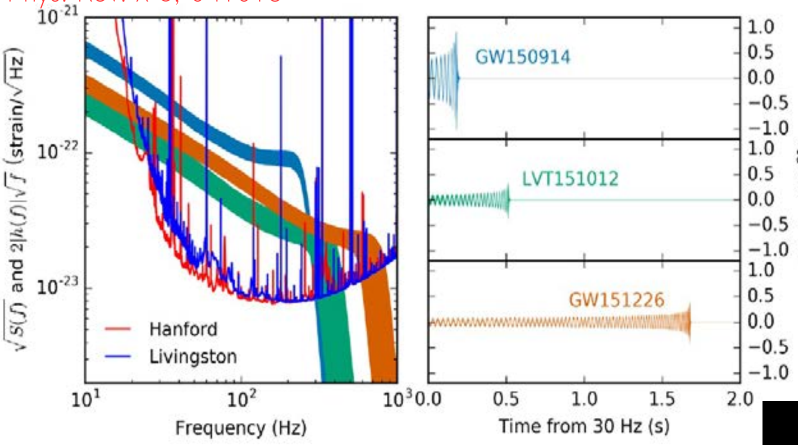

GW150914 (significance >5.3σ)
LVT151012 (Candidate 1.7σ)
GW151226 (significance>5.3σ)

Amplitude spectral density of the total strain noise of the H1 and L1 and the recovered signals

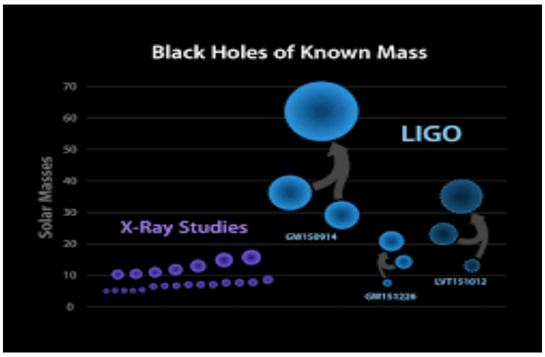

GW150914 - September 14, 2015 at 09:50:45UTC
✗ 29 and 36 Msun
✗ Duration ~ 0.2s
GW151226 December 26, 2015 at 03:38:53 UTC
✗ 7 and 14 Msun
✗ Duration ~ 1s

O1 analysis: first detection

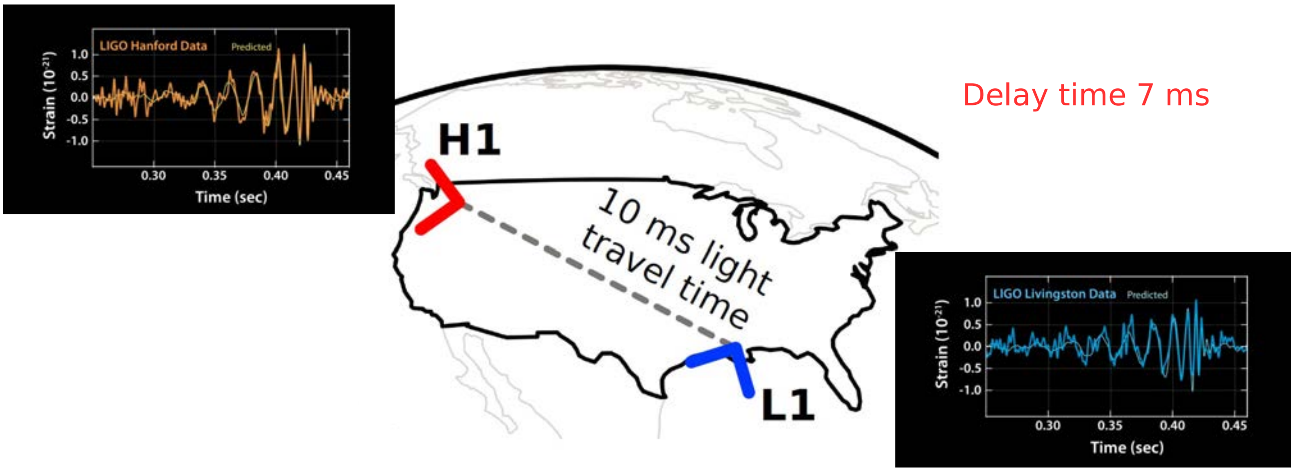

Delay time 7 ms

- ✗ 3 minutes alert from the low latency searches pipeline coherent Wave Burst (cWB) (Florida, Hannover, Padova/Trento)
- ✗ Two independent sky maps available in short time (cWB 17 min, LIB 14 hours) within 600 deg^2 (90% c.l.)
- ✗ As the preliminary estimate of the event significance overcomes the planned threshold (1/month) within 48 hours, allert sent via GCN circular to 62 astronomer partners (including INAF PD).

O1 analysis: first detection, confidence

The possibility that the transient GW150914 is due to environmental or instrumental excess noise is ruled out. 5.1 evidence of the astrophysical origin of the signal

Two independent data analysis pipelines used to estimate the confidential level

Template search,	Generic (burst) search,
Estimated False Alarm rates: <1/203000 years	Estimated False Alarm rates: <1/225000 years

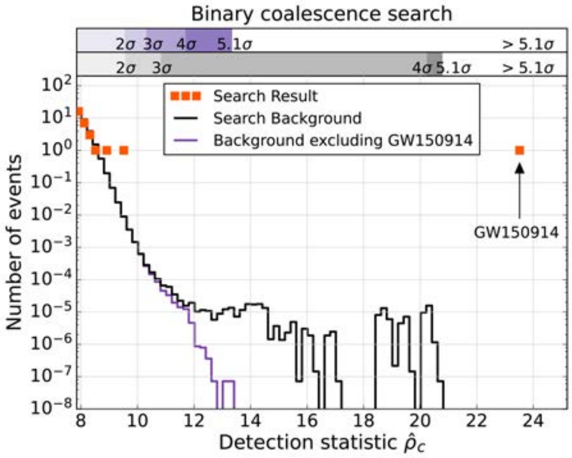

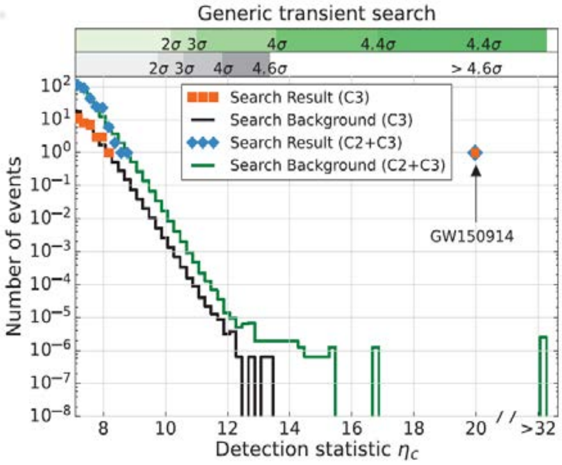

O1 analysis: first detection, binary parameters

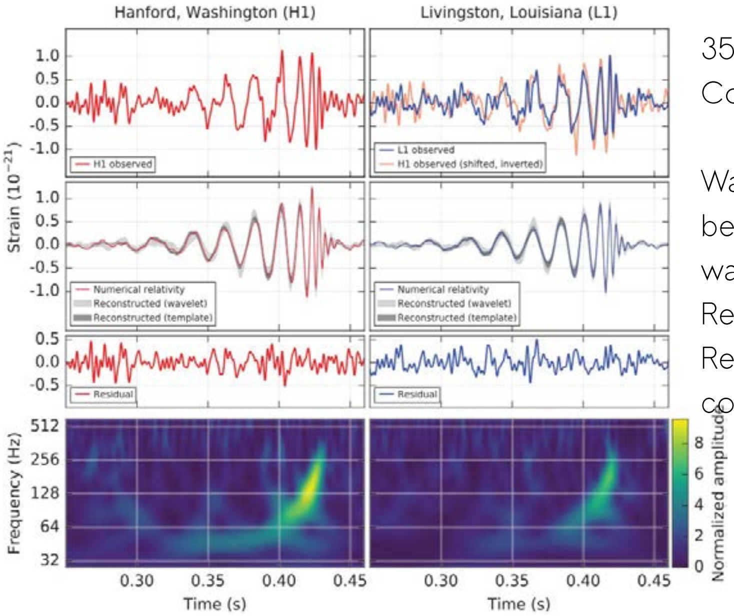

35 - 350 Hz band-passed strain time series. Coherent signals in both detectors

Waveform reconstruction, agreement between best fit theoretical waveforms, wavelet (unmodeled) and NR (Numerical Relativity)

Residual noise after waveform subtraction consistent with instrumental noise

Mass 1	$36.3^{+5.3}_{-4.5} M_\odot$
Mass 2	$28.6^{+4.4}_{-4.2} M_\odot$
Final mass	$62.0^{+4.4}_{-4.0} M_\odot$
Energy radiated in GW	$3.0^{+0.5}_{-0.5} M_\odot$
Spin magnitude $\|a1\|$	$0.32^{+0.45}_{-0.28}$
Spin magnitude $\|a2\|$	$0.57^{+0.40}_{-0.51}$
Final spin $\|a_f\|$	$0.67^{+0.06}_{-0.08}$
Luminosity distance	$410^{+160}_{-180} Mpc$

- ✗ The physical system is described by 8 parameters: $m_{1,2}$ and $S_{1,2}$
- ✗ 9 additional parameters are required Luminosity distance, celestial coordinates, orbit inclination, time and phase of coalescence.

O1 analysis: first detection, follow up

Electromagnetic follow up.

Covered sky map (contained probabillity):

GW

Gamma-ray: 100 %

Optical: over 50 %

Radio: 86 %

X-ray: 90 %

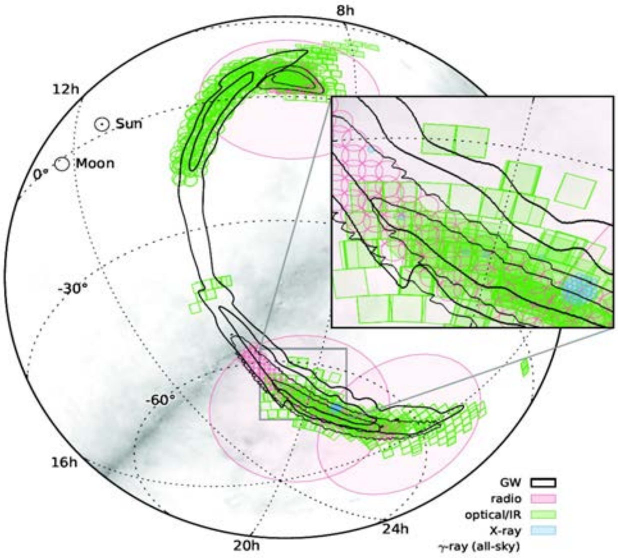

Neutrino joint analysis

Search for coincident neutrino candidates of IceCube and ANTARES (in 500s window):

-ANTARSE: 0 neutrino candidates:

-IceCube: : 3neutrino candidates, consistent with the expected background (No one directionally coincident with GW150914)

Interferometers network, second generation

Living Reviews in Relativity DOI 10.1007/lrr-2016-1

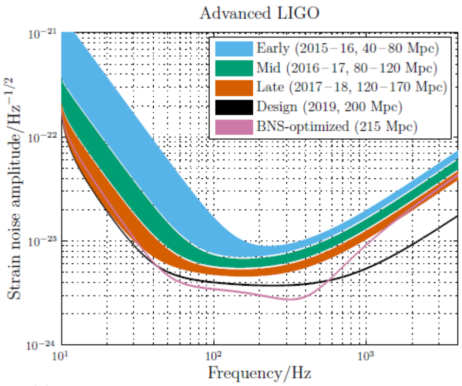

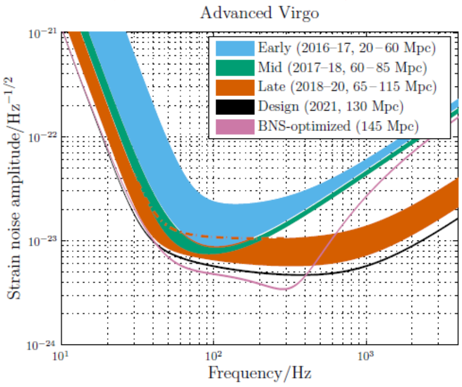

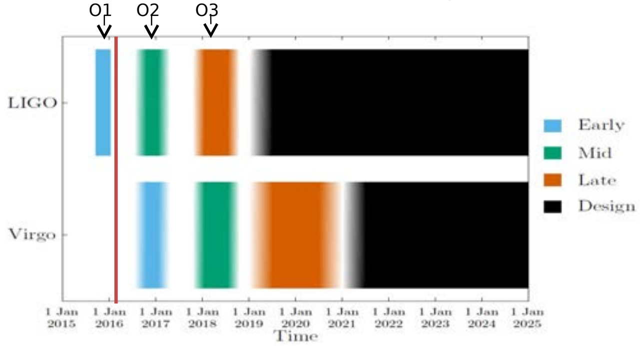

- Estimated BNS detection rate: 0.2-200 per year
- Sky position ~5 deg^2

Three detector localization

Living Reviews in Relativity DOI 10.1007/lrr-2016-1

Face-on BNS
80 Mpc

2016-2017

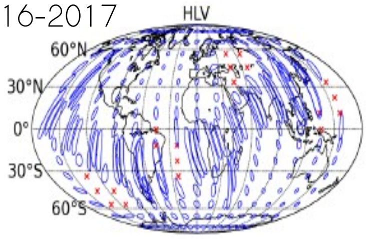

2017-2018

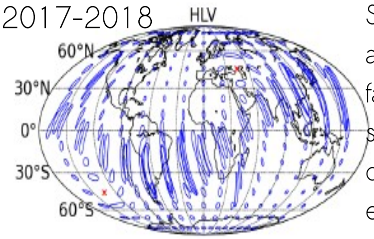

Face-on BNS
160 Mpc

2019+

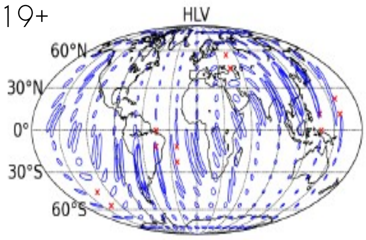

2022

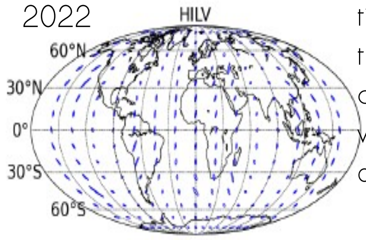

Schematic network sensitivity and localization accuracy for face-on BNS systems with advanced-detector networks. The ellipses show 90% confidence localization areas based upon timing triangulation alone, and the red crosses show regions of the sky where the signal would not be confidently detected.

GW150914

L1H1:600 deg^2
If Virgo: L1H1V1: 90% probability sky area reduced by a factor 30

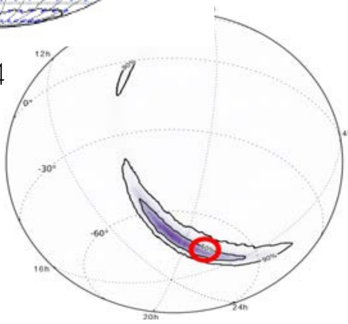

GW spectrum

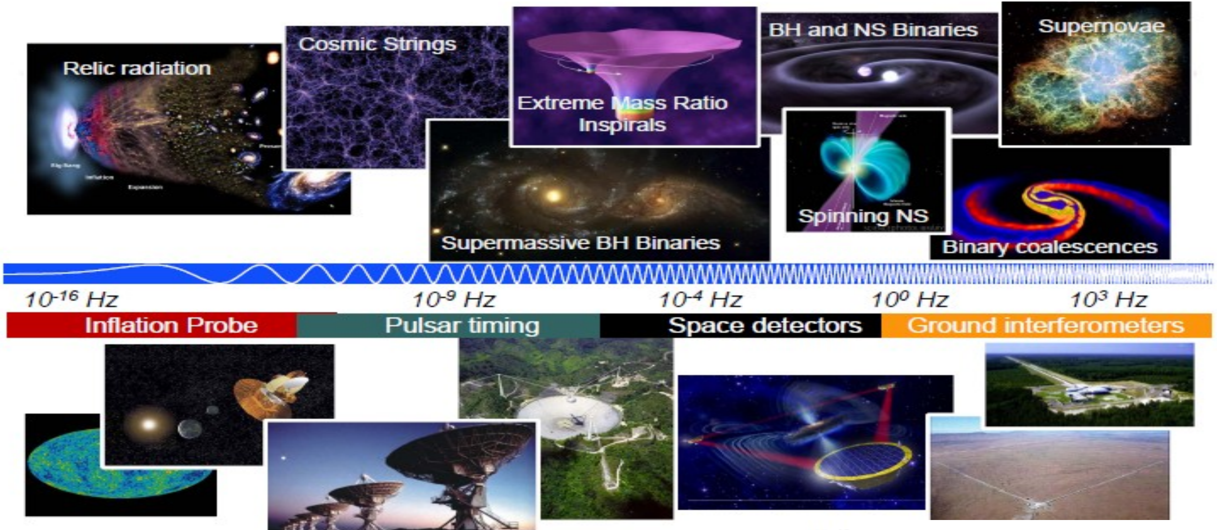

to "be sensitive" to GW spectrum:

- ✗ improve ground interferometers
- ✗ space interferometers

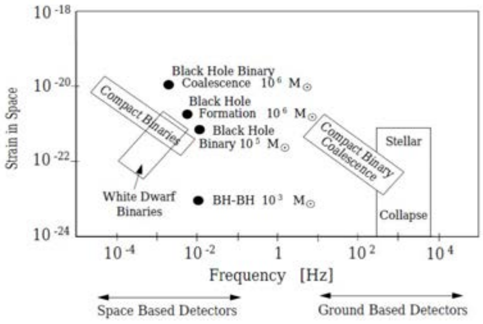

Future

"Limit" to improvement of the second generation interferometer: length of the arms, seismic and newtonian noise, size of the beam (thermal noise), :

"3rd generation observatory":

- ✗ Possible new technology: squeezed light, alternative wavelengths + cryogenics, longer arms, go underground (access low frequencies)
- ✗ Factor ~10 sensitivity increase over aLIGO (10 Hz - few kHz); sensitivity x10 ⇒volume x10^3
- ✗ Low frequency sensitivity (down to ~ 5 Hz)

Einstein telescope design studies

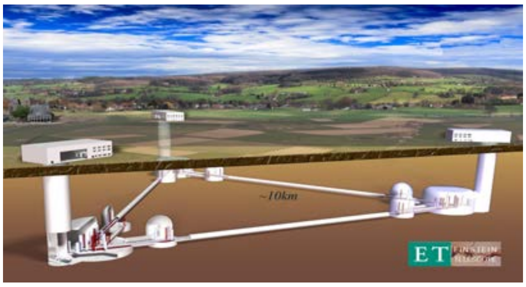

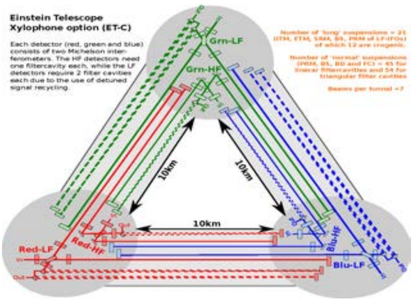

- ✗ 10 km arm length
- ✗ Underground, cryogenics
- ✗ New geometries or topologies, multiple interferometers

Space interferometers

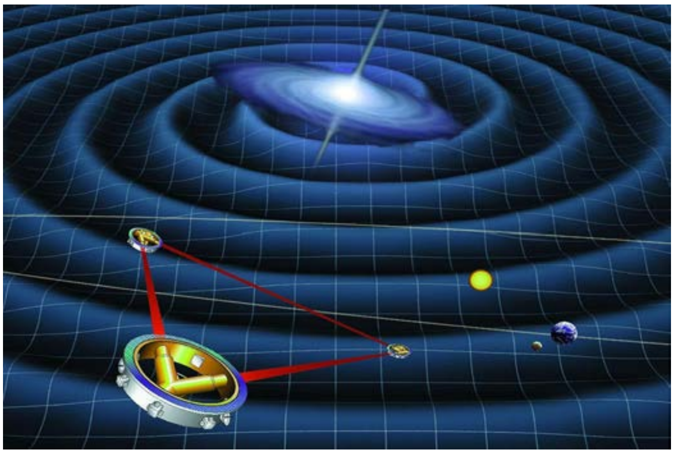

✗ 3 Spacecraft 2.5 Million-km arm-lengths
✗ Test masses in sub-femto-g free fall ($10^{-15}\,\mathrm{m/s^2/\sqrt{Hz}}$)
✗ Laser interferometry between TMs

Successful LISA Pathfinder mission
Mission proposal submitted (arXiv:1702:00786)
Launch 2030-2034

Possible source:
massive black hole binaries (MBHBs) detection, parameter estimation..and MBH formation.
Extreme mass ratio inspirals (EMRIs)
Cosmological background

Back up

Detector Characterization

Non-stationary and non-Gaussian, zoo of instrumental glitches background has heavy tails

Many potential sources of uncorrelated noise (anthropogenic noise, earthquakes, radio frequency modulation). Random coincidences can generate coherent events, transient noise (glitches) can occur within the targeted frequency range

LIGO detectors record over 200000 auxiliary channels to monitor instrument behavior and environmental conditions

Auxiliary channels witness possible coupling mechanisms: check for systematic correlations with h(t) gravitational channel

Blip glitches: short noise transient, without clear correlation to any auxiliary channels

arXiv: 1602.03844

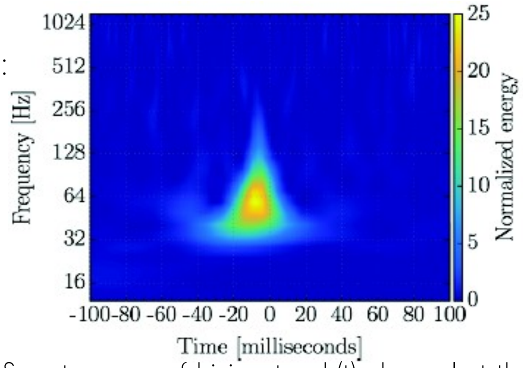

Spectrogram of Livingston h(t) channel at the time of blip glitch

---

Localization GW150914

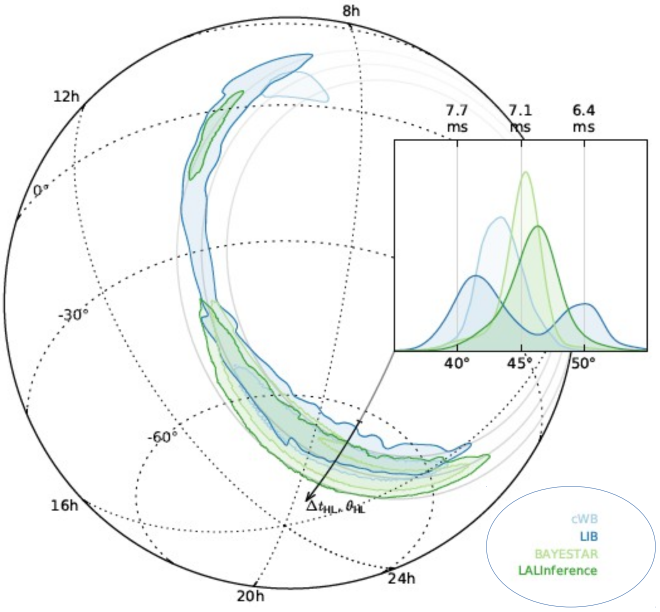

Background estimation

Significance of an event : is determined by the rate at which the detector noise produces events (**background**) with detection statistic greater or equal to the one of the event
The background is not uniform across the parameter space of the searched signals

Background estimation procedure:

✗ Apply non-physical (> 1 s) time-shifts to data stream and repeat analysis
✗ Estimate reference background distribution of noise-only events
✗ Compare distribution of non time-shifted (“zero-lag”, “real data analysis ”) events to reference to get confidence (probability of occurrence) (Limit on of the number of time-slides available

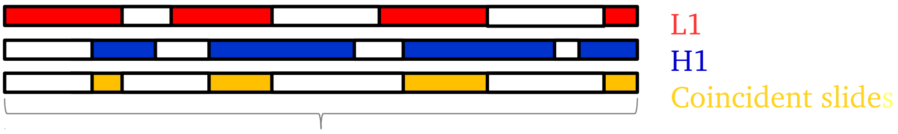

Analysis -> Candidate events

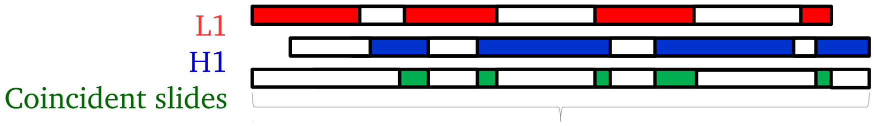

Analysis -> Background events

Template CBC

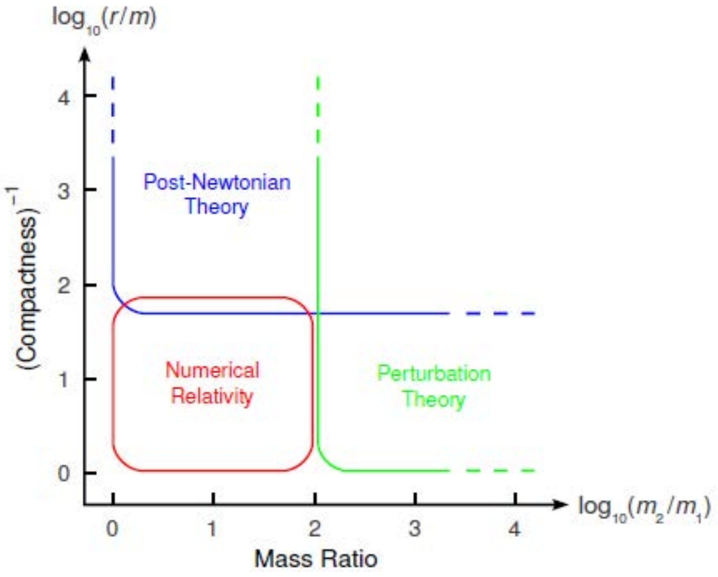

LIGO sensitivity O1

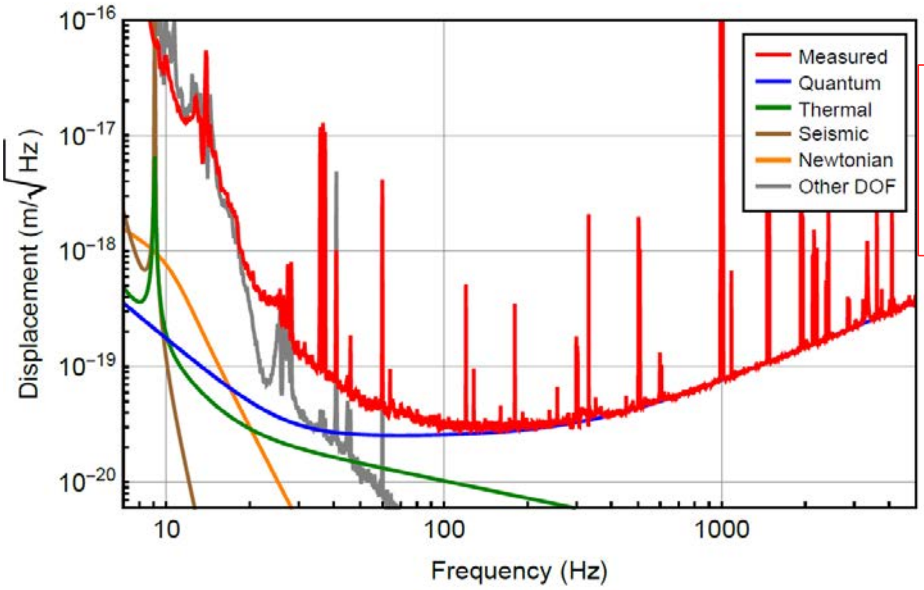

GW150914: The Advanced LIGO Detectors in the Era of FirstDiscoveries (Phys. Rev. Lett. 116,131103)

The displacement sensitivity of the Advanced LIGO detector in Hanford during the first observation run O1. The sum of all known noise sources accounts for most of the observed noise with the exception of the frequency band between 20 Hz and 100 Hz.